Theor Chem Acc (1998) 99:301–311
DOI 10.1007/s002149800m16

Theoretical
Chemistry Accounts

Regular article

Gas phase and water solution conformational analysis of the herbicide diuron (DCMU): an ab initio study

Hélio F. Dos Santos[1], **Patrick J. O'Malley**[2], **Wagner B. De Almeida**[1]

[1] Laboratório de Química Computacional e Modelagem Molecular (LQC-MM), Departamento de Química, ICEx, U.F.M.G., Belo Horizonte, MG, 31270-901, Brazil
[2] Department of Chemistry, U.M.I.S.T., P O Box 88, Manchester M60 1QD, UK

Received: 23 February 1998 / Accepted: 28 May 1998 / Published online: 19 August 1998

Abstract. In the present work, the conformational equilibrium for the herbicide diuron (DCMU) has been investigated using high level ab initio calculations. The solvent effect was included through two different continuum models: (1) the real cavity IPCM method and (2) the standard dipole Onsager model SCRF. The effect due to solute-solvent hydrogen-bond interactions was analyzed considering a hybrid discreet-continuum model. At the Hartree-Fock level, the gas phase results showed that only the *trans* forms (A and B) are present in the equilibrium mixture, with the relative concentrations found to be 33% (A) and 67% (B) (HF/6-311 + G**//6-31G**). When the electronic correlation effect is included (MP2/6-31G*//HF/6-31G*), a relative stabilization of the *cis* forms was observed, with the conformational distribution calculated as 38% (A), 50% (B), 6% (C) and 6% (D). The *trans* conformations were found to be completely planar, which has been considered to be a prerequisite for the herbicide binding. In water solution, the *trans* conformation A should be the most abundant conformer, the IPCM and SCRF values being ca. 100% and ca. 85% respectively. The IPCM calculations with the isodensity level set to 0.0005 present a conformational distribution close to that obtained from the hybrid model [92% (A) and 8% (B)], which has been considered our best solvent approach. Regarding the biological action of urea-type herbicides, the results presented here are important, because some QSAR studies have suggested that the partition coefficient is related to the herbicide activity, so the conformational equilibrium may play a role in the biological action.

Key words: DCMU – Diuron – Conformational analysis – Solvent effect – Ab initio calculation

Correspondence to: H.F. Dos Santos

1 Introduction

The electron transport involved in the light phase of photosynthesis in plants occurs through the action of two photosynthetic reaction centers named photosystem I (PSI) and photosystem II (PSII). These systems are constituted of protein complexes associated with the thylakoid membrane and are connected by another transmembrane protein called cytochrome b_6f complex (cyt-b_6f). In this mechanistic model (known as Z-scheme), the electrons are transferred between these protein complexes via a mobile electron carrier [1]. Many common herbicides interfere in the electron flow from PSII to cyt-b_6f. They compete with the secondary electron acceptor plastoquinone (Q_B) for the binding site on PSII, blocking the reduction process of Q_B by the reduced primary quinone Q_A and consequently interrupting the electron-transport chain [1].

The structural information obtained from purple bacteria has contributed to the elucidation of the constitution of the PSII reaction center (RC) [2]. From homology studies between protein sequences of photosynthetic bacteria and PSII, the so-called Q_B site has been identified as being located on a 32 kDa protein known as the D1 subunit [2]. The use of inhibitor and mutants of the protein subunits has allowed the identification of the exact Q_B and the herbicide binding domain [3]. The decisive step in the elucidation of the structure of PSII was the resolution of the crystalline structure of the protein subunits in the photosynthetic RC of *Rhodopseudomonas viridis* [4], which has been useful for modeling the PSII reaction center [5].

Belonging to the class of classical photosynthetic inhibitors, the substituted aryl-ureas were the first group of highly effective herbicides and were introduced in 1956 [6]. As triazines and phenolics, the urea-type inhibitors act by blocking the oxidation of the reduced primary quinone Q_A by Q_B. The parent compound of the urea-type derivatives (DCMU, [3-(3,4-dichlorophenyl)-1,1-dimethylurea]) has been used as probe in some

studies with the aim of identifying the amino acids involved in the herbicide binding and the nature of the interactions [5, 7].

The nature and topography of the binding site of the inhibitor is naturally of great importance for attempts to rationalize the design of new and better herbicides. On the other hand, knowledge of the molecular structure and properties of the ligand can provide useful information that can help in understanding the ligand-receptor interaction and consequently the biological activity. This is the basis of the classical quantitative structure-activity relationship (QSAR), which has as a paradigm the description of the biological response by physical-chemical parameters derived from the ligand structures. In a recent review, Hansch and Leo [8] reported the most important and significant pesticide QSAR. Related to the urea-type photosynthetic inhibitors, the best QSAR study shows a bilinear [9] dependence on log P [8] (P is the partition coefficient in octanol/water), $\log P_0 = 5.07$ being the ideal value (maximum biological potency) (the DCMU derivative has $\log P = 2.80$ [8]). Another QSAR study, reported by Hansch and Leo [8], on *N*,*N*-dimethyl-*N*′-phenylurea suggests some electronic contribution to activity. This QSAR model was developed considering the lipophilicity parameter π and the electronic parameter σ and it was observed that electron-withdrawing substituents at the phenyl ring increase the biological potency. With the improvement of computers and theoretical molecular orbital models, quantum chemical descriptors have been applied in the construction of QSAR models [10]. In that line of study, the first step is the establishment of the probable conformations of the molecule, which are located through investigation of the multidimensional potential energy surface (PES). Some recent studies related to theoretical conformational analysis of compounds with biological interest can be found in [11–15].

In previous studies, quantum mechanical semiempirical methods [11, 12, 16, 17] and empirical force fields [12, 17] have been applied for the investigation of the PES for PSII inhibitors. All those studies were concerned with the determination of structure and molecular properties of the molecules and the calculation of the quantities related to the conformational equilibrium. In the present work, we investigate the conformations and electronic parameters of the DCMU herbicide using high level ab initio molecular orbital calculations. The gas phase and water solution properties have been investigated and the conformational equilibrium analyzed.

2 Calculations

In our previous work [12], we carried out a systematic conformational analysis for the DCMU compound (Fig. 1) using different quantum mechanical semiempirical methods (AM1 and PM3) and molecular mechanics empirical model MM2/MMX. In that study, the PES for the DCMU molecule was obtained by successive rotations around the C—N bonds (see Fig. 1). The results showed four distinct minimum energy conformers as stable forms of the DCMU molecule. The transition

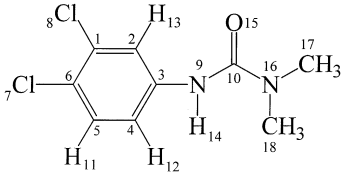

Fig. 1. Specification of the atomic labels and numbering scheme for the DCMU molecule and definition of the main dihedral angles: ω_1: [H_{14}, N_9, C_3, C_2], ω_{11}: [C_{10}, N_9, C_3, C_4] ω_2: [O_{15}, C_{10}, N_9, C_3], ω_{22}: [N_{16}, C_{10}, N_9, H_{14}], ω_3: [C_{17}, N_{16}, C_{10}, C_9], ω_{33}: [C_{18}, N_{16}, C_{10}, O_{15}]

state structures connecting the minima on the PES, were also obtained and characterised as first order transition states through harmonic frequency analysis.

In the present study, the stationary points located on the AM1 PES [12] were used as starting guesses in the ab initio geometry optimization. Firstly, the geometry optimization was carried out at the Hartree-Fock (HF) level of theory using the following basis sets: 3-21G*, 6-31G*, 6-31 + G* and 6-31G**. In the HF/3-21G*, HF/6-31G* and HF/6-31 + G* calculations, the polarization functions were included only on the chlorine atoms. In a second part of the study, the energy was calculated at the HF/6-311 + + G**//6-31G** level of theory and the electronic correlation effect was taken into account through MP2 (Møller-Plesset second-order perturbation theory) single point calculations, designated MP2/6-31G*//HF/6-31G*.

The solvent effect was analyzed using two distinct continuum models, the isodensity polarized continuum model (IPCM) [18] and the standard Onsager self-consistent reaction field (SCRF) methodology [19] with the inclusion of only the dipole term in the electrostatic potential expansion [20]. The dielectric constant of water, $\varepsilon = 78.54$, was used in all solvent calculations. The structural contribution to the solvation process was calculated from the geometry optimization in the presence of the dielectric medium (SCRF dipole model).

The hydrogen bond contribution to the solvation energy was taken into account in the last part of this study. It was included considering the following reaction:

$$H_2O + H_2O + DCMU_i \rightarrow DCMU_i \ldots (H_2O)_2 \qquad (1)$$

where $DCMU_i$ specifies the distinct conformations of the molecule. The solvation free energy was calculated from

$$\Delta G_i^{solv} = n\Delta G^{vap}(H_2O) + \Delta G^{ass}(DCMU_i \ldots (H_2O)_2) + \Delta G^{pol}(DCMU_i \ldots (H_2O)_2) \qquad (2)$$

as proposed by Li and coworkers [21]. In Eq. (2), ΔG^{vap} (H_2O) is the experimental vaporization energy of water (6.3 kcal/mol [22]). ΔG^{ass} ($DCMU_i \ldots (H_2O)_2$) corresponds to the complexation free energy for process (1) and ΔG^{pol} ($DCMU_i \ldots (H_2O)_2$) is the polarization energy taken from the Onsager SCRF continuum model.

All the calculations were carried out using the GAUSSIAN-94 [23] program at the Laboratório de Química Computacional e Modelagem Molecular

(LQC-MM) of the Departamento de Química, Universidade Federal de Minas Gerais (UFMG).

3. Results and discussion

3.1 Gas phase

The main geometric parameters for the distinct conformations of the DCMU molecule are shown in Table 1. The values obtained from different levels of theory and the dihedral angles derived from the crystal structure [24] are reported. The HF/6-31G** fully optimized geometries of conformers A–D are depicted in Fig. 2. The conformations A and B are classified as *trans* and C and D as *cis* according to the relative position of the N—H and C═O groups, which are defined by the torsion angles ω_2 and ω_{22} (Table 1). From these results, it can be seen that the *trans* forms of the herbicide DCMU are completely planar in all calculations. The angle between the substituted phenyl ring and the dimethylurea moiety (ω_1 and ω_{11}) is close to 180° and 0°, respectively for conformers A and B. The solid state structure [24] showed a nonplanar *trans* conformation (similar to our conformer B) with ω_1 and ω_{11} twisted by 28.3° and 29.4° respectively. This can be explained through the analysis of the net-crystalline interactions, which should favor a hydrogen bond between the N—H of one molecule and the C═O group of the other. Figure 3 shows a representation of three molecules present in the crystal of the herbicide DCMU. The spatial positions are defined by $(x - 1/2, -y + 1/2, z)$, (x, y, z) and $(x + 1/2, -y + 1/2, z)$, where x, y and z are the crystallographic coordinates [24]. From this analysis, it was found that the N...O and H...O distances are 2.936 and 1.959 Å respectively. Despite the greater electronic conjugation, one factor that might be responsible for the stabilization of the planar forms in the isolated system is the presence of an attractive electrostatic interaction between the phenyl hydrogens H_{13} (A) and H_{12} (B) with the carbonyl group. The H...O distances, calculated at the HF/6-31G** level, were found to be 2.174 (A) and 2.182 Å (B). A twisted conformation for the DCMU molecule, similar to the solid state structure, was obtained in our previous study [12] using semiempirical and molecular mechanics methods. The crystallographic geometry was used as an initial guess in the ab initio optimization procedure. The fully optimized structure obtained for all basis sets considered in the present study was the planar conformer B (Fig. 2b), showing that the twisted conformation does not correspond to a stationary point on the ab initio PES for the DCMU compound at the level of theory used in this study. The total energy of the nonplanar conformer was calculated at HF/6-31G** level with the dihedral angles ω_1 and ω_{11} fixed at the values obtained from the X-ray study (28.3° and 29.4° respectively). The result showed that the *trans* twisted from is only 0.327 kcal/mol higher in energy than the corresponding planar conformer (B). This small energy difference can be used to explain the fact that the weak hydrogen bonds present in the crystalline net are enough to twist the conformation (see Fig. 3).

The dihedral angles presented in Table 1 show that the *cis* forms are more sensitive to the basis set used than

Table 1. Optimized dihedral angles for the different conformations of the DCMU molecule obtained in the gas phase. The X-ray data are included for comparison

		Dihedral angles (degree)[a]					
		ω_1	ω_{11}	ω_2	ω_{22}	ω_3	ω_{33}
		H_{14}–N_9–C_3–C_2	C_{10}–N_9–C_3–C_4	O_{15}–C_{10}–N_9–C_3	N_{16}–C_{10}–N_9–H_{14}	C_{17}–N_{16}–C_{10}–N_9	C_{18}–N_{16}–C_{10}–O_{15}
A	HF/3-21G*	180.0	−179.9	0.1	0.2	−179.8	−179.9
	HF/6-31G*	180.0	−179.9	0.1	0.1	−179.9	−179.9
	HF/6-31+G*	180.0	180.0	0.1	0.1	−179.9	−179.9
	HF/6-31G**	180.0	−179.9	0.0	0.1	−179.9	180.0
B	HF/3-21G*	0.0	0.1	0.1	0.2	−179.9	−179.9
	HF/6-31G*	0.0	0.1	0.1	0.1	−179.9	180.0
	HF/6-31+G*	0.0	0.1	0.1	0.1	−179.9	180.0
	HF/6-31G**	0.0	0.1	0.0	0.1	−179.9	180.0
C	HF/3-21G*	40.5	20.4	−143.7	−165.5	−171.0	−146.1
	HF/6-31G*	48.3	28.2	−143.8	−165.1	−170.2	−152.5
	HF/6-31+G*	52.0	30.1	−142.7	−165.3	−170.4	−154.1
	HF/6-31G**	54.1	19.7	−138.1	−172.6	−175.8	−146.3
D	HF/3-21G*	140.0	164.8	143.7	165.4	170.8	145.4
	HF/6-31G*	131.4	156.7	144.0	165.0	170.1	152.2
	HF/6-31+G*	128.1	154.8	143.0	165.1	170.3	153.8
	HF/6-31G**	128.0	165.9	138.0	172.1	175.7	146.1
	X-ray[b]	28.3	29.4	2.6	0.5	−175.5	−174.0

[a] See Fig. 1 for the numbering scheme
[b] Data taken from [24]

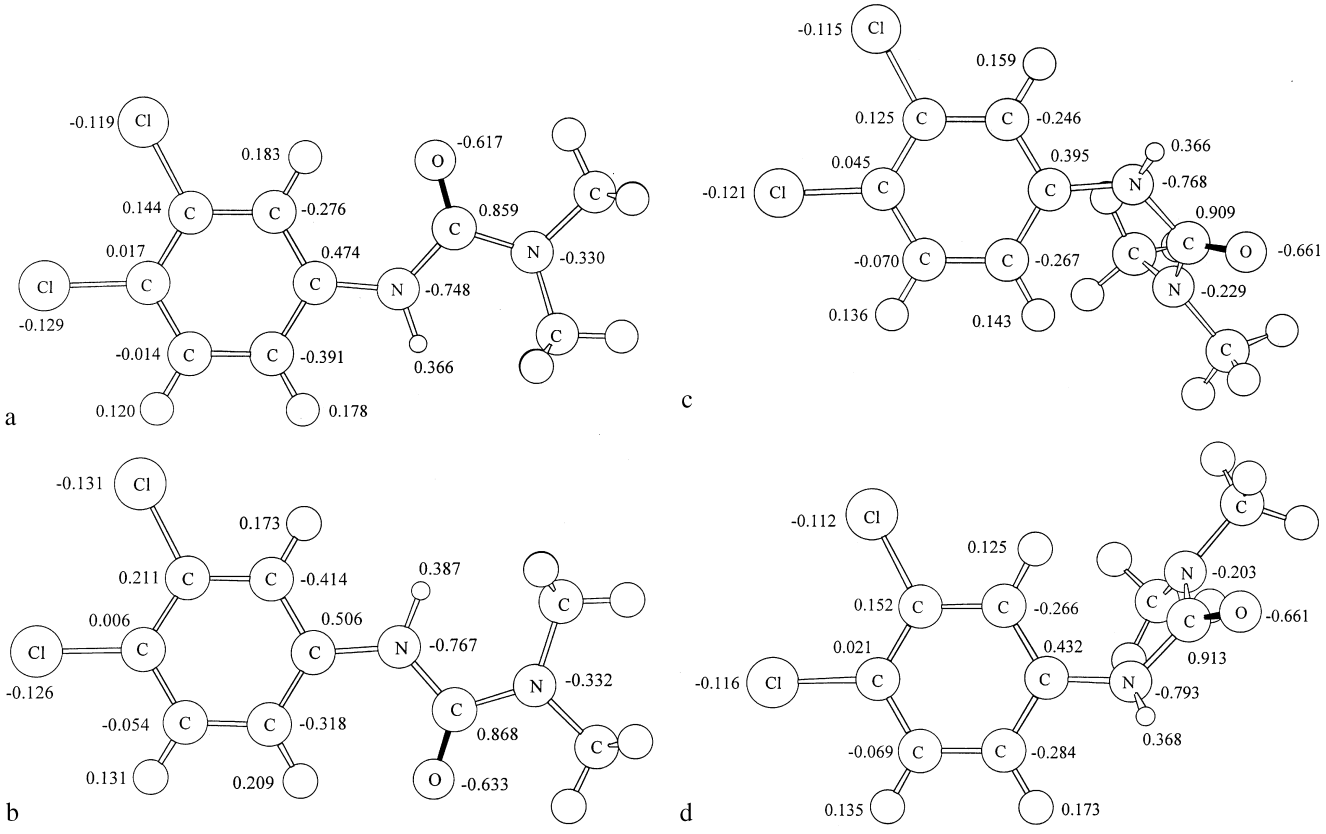

Fig. 2a–d. HF/6-31G** fully optimized geometries for the minimum energy structures A–D located on the PES for the herbicide diuron (DCMU). The atomic charges (CHELPG) are also presented

the *trans* conformations. For conformers C and D, a less planar form was observed with the improvement of the basis set (see Table 1).

The herbicide activity of the DCMU derivative has been attributed to the *trans* forms [5, 7, 16, 17], possibly through a double hydrogen bond involving the N—H (donor) and C=O (acceptor) groups. However, the participation of the *cis* conformer in the interaction with the photosynthetic reaction center has been discussed using, as a template, lenacil (a uracil derivative) [17], where the H—N—C=O peptide group is forced into the *cis* form by the cyclic structure. The O...H distance in lenacil is 2.4 Å and this distance was calculated at the HF/6-31G** level to be 2.316 (C) and 2.313 Å (D). The geometries of conformers C and D are represented in Fig. 2c and d respectively.

According to molecular modeling studies [4, 5], the main attractive interactions between the herbicide and the Q_B site involve hydrogen bonds of the phenylamino NH group with the side chain of Ser264 or Ser268 and the peptide carbonyl oxygen of Ala251. Therefore, the acidity of the hydrogen of the H—N—C=O group in the DCMU molecule should be considered as an important quantitative parameter to be correlated with the biological response. It has been demonstrated in a QSAR study [17] involving phenyl-urea derivatives that the MNDO net-charge of the N—H hydrogen is correlated with the half-inhibitory concentration in triazine susceptible chloroplast (I_{50}), the values of q_H and I_{50} being equal to: 0.1954, 0.05 (diuron), 0.1927, 0.35 (monuron) and 0.1900, 3.20 (fenuron). This result shows that the hydrogen acidity is proportional to the herbicide activity. The values of the electrostatic derived charges, obtained from the HF/6-31G** calculation, are given in Fig. 2. It can be seen that the most positive hydrogen

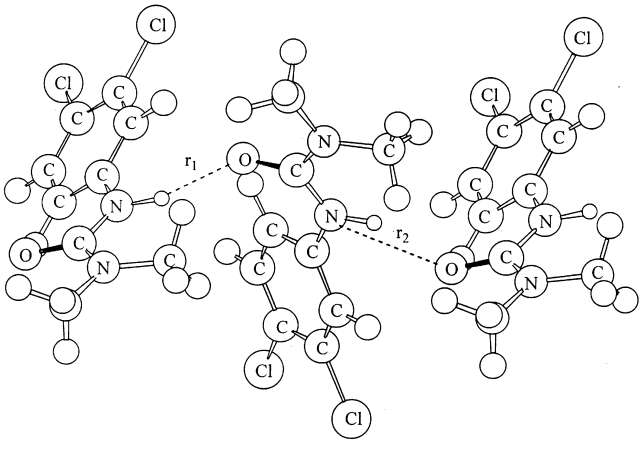

Fig. 3. Representation of three molecules present in the crystal of the DCMU molecule, showing the hydrogen bonds which should be responsible for the twisting in the solid state structure. The respective crystallographic position are: $(x - 1/2, -y + 1/2, z)$, (x, y, z) and $(x + 1/2, -y + 1/2, z)$. The values of r_1(H...O) and r_2(N...O) are 1.959 and 2.936 Å respectively

charge was calculated for the N—H hydrogen of conformer B ($qH_{14} = 0.3869$), which is more available to form a hydrogen bond. The atomic charges obtained from other levels of theory show the same qualitative trend.

Table 2 presents the relative Gibbs free energy change for the four stable conformations of the DCMU molecule. The conformational distribution, calculated at 298 K, is also reported. The values in Table 2 show that the *trans* from B corresponds to the global energy minimum on the PES for the herbicide diuron at all levels of calculation. At the HF level, the free energy differences were found to be lower than 0.5 kcal/mol between *trans* conformations and higher than 3.8 kcal/mol between *trans* and *cis* conformers. The lower value for ΔG(*trans*-*trans*) (= 0.225 kcal/mol) and the highest for ΔE(*cis*-*trans*) (= 6.125 kcal/mol) were observed at the lowest level of calculation (HF/3-21G*). According to the results obtained, a relative stabilization of the C and D conformers with the increase of the basis set used is observed. At the HF/6-311++G**//6-31G** level, the C and D *cis* conformers are only 3.8 kcal/mol higher in energy than the *trans* form B. The population analysis in Table 2 shows that even at the highest HF level of theory, the *cis* conformations should not be present in a significant ratio in the gas phase. However, when the electronic correlation is taken into account through MP2/6-31G*//HF/6-31G* single point calculations, the *cis* forms were found to be present in a relative concentration of 6%. The Gibbs population shows that the relative concentration of conformer A is slightly increased, but the population of conformation B drops from 66% (HF/6-31G*) to 50% (MP2/6-31G*//HF/6-31G*).

The biological activity is strongly dependent on the molecular conformations of the active compound. However, the possible conformers and the easiness of the interconversion process should be considered as important parameters for describing the biological action. For the herbicide Swep, the properties related to the conformational equilibrium have been used to explain the low activity of this phenylcarbamate inhibitor [17]. For this compound, the *cis* form was found to be only 1.5 kcal/mol higher in energy than the *trans* conformation, with the energy barrier being equal to 2.5 kcal/mol, which allows a flip-flop between the *cis* and *trans* forms. Analyzing our results from a thermodynamic point of view, it can be observed that at the MP2/6-31G*//HF/6-31G* level, both *cis* conformations are likely to exist in the conformational mixture (Table 2). The kinetics of the process can be analyzed from the calculation of the energy barriers involved in the conformational interconversions. For the DCMU molecule, the interconversion process can be divided into four steps: (1) A → B (*trans* → *trans*), (2) B → C (*trans* → *cis*), (3) C → D (*cis* → *cis*) and (4) D → A (*cis* → *trans*). Processes 1 and 3 involve a rotation around the C (Ph) —N bond and processes 2 and 4 occur via a rotation about the C(=O)—N bond of the peptide group. The transition state (TS) geometries connecting the stable conformers were located on the PES and fully optimized using different ab initio levels. The harmonic frequencies were calculated in order to characterize the stationary point as a first order transition state. The HF/6–31G** optimized structures are represented in Fig. 4. The gas phase calculated energy barriers are reported in Table 3. From the values reported in Table 3, it can be observed that the *trans* → *cis* (2) and *cis* → *trans* (4) energy barriers were found to be higher than the values calculated

Table 2. Relative Gibbs free energies (in kcal mol^{-1}) and conformational populations (at 298 K) for the minimum energy structures of the diuron molecule obtained in the gas phase

	Conformations[a]			
	A	B	C	D
HF/3-21G*				
ΔG[c]	0.225	0.000	6.126	6.125
[Gibbs][d]	41%	59%	0%	0%
HF/6-31G*[b]				
ΔG[c]	0.381	0.000	5.462	5.493
[Gibbs][d]	34%	66%	0%	0%
HF/6-31+G*[b]				
ΔG[c]	0.319	0.000	4.640	4.626
[Gibbs][d]	37%	63%	0%	0%
HF/6-31G**[b]				
ΔG[c]	0.471	0.000	4.127	4.197
[Gibbs][d]	31%	69%	0%	0%
HF/6-311++G**//6-31G**				
ΔG[c,e]	0.414	0.000	3.826	3.813
[Gibbs][d]	33%	67%	0%	0%
MP2/6-31G*//HF/6-31G*				
ΔG[c,e]	0.173	0.000	1.309	1.208
[Gibbs][d]	38%	50%	6%	6%

[a] The main structural parameters are presented in Table 1
[b] The frequencies were scaled with the factor 0.8929 according to [28]
[c] $\Delta G = \Delta H - T\Delta S + \Delta ZPE$
[d] $\Delta G_{ij} = -RT\ln(n_i/n_j)$, R being the gas constant and T the absolute temperature (= 298 K)
[e] The ΔG values were calculated considering the thermal correction to the Gibbs free energy from the HF/6-31G** and HF/6-31G* calculations respectively

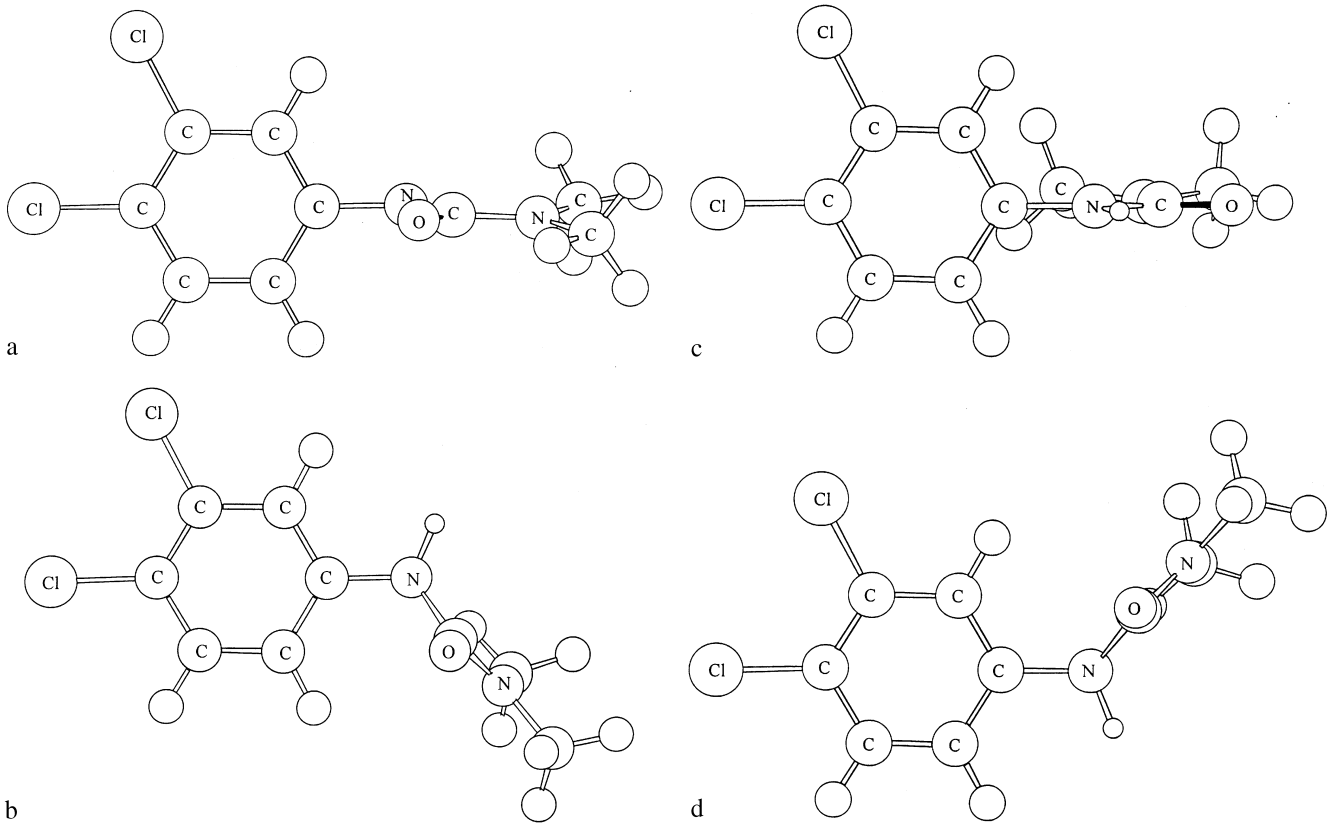

Fig. 4a–d. HF/6-31G** fully optimized geometries for the transition state structures TS_{AB}–TS_{DA} connecting the different conformations on the PES for the herbicide diuron (DCMU). The dihedral angle involved in the internal rotation are: TS_{AB} : $w_{\perp} = 103°$, $w_{11} = -82.6°$; TS_{BC} : $w_2 = -60.4°$, $w_{22} = -111°$; TS_{CD} : $w_{\perp} = 92.5°$, $w_{11} = 96.4°$; TS_{DA} : $w_2 = 59.0°$, $w_{22} = -109.9°$

for the interconversion (1) and (3). For the B → C process, the value of the energy barrier was significantly affected by the choice of the basis set, the highest value being that calculated using HF/3-21G* (12.323 kcal/mol) and the lowest value was found using MP2/6-31G*//HF/6-31G* (7.098 kcal/mol). However, the barrier obtained from the MP2 calculation is still high enough to avoid the flip-flop between the *cis* and *trans* conformations. A similar result was obtained for the A → B process, where it was observed that the energy barrier drops from 5.8 (HF/3-21G*) to 2.5 kcal/mol (MP2/6-31G*//HF/6-31G*), the lowest value being calculated at HF/6-311++G**//6-31G** level (1.987 kcal/mol). The changes in the interconversion barriers for the C → D and D → A process are small, being close to 5 and 6 kcal/mol, respectively.

3.2 Water solution

As mentioned in the Introduction, QSAR studies of herbicide species suggest that the partition coefficient plays a role in the biological activity of phenyl-urea derivatives [8]. Therefore, it is important to investigate

Table 3. Conformational interconversion barriers for the DCMU molecule in the gas phase

	$\Delta E_{ij} = E(TS_{ij}) - E_i$/kcal mol^{-1}			
	A → B	B → C	C → D	D → A
HF/3-21G*	5.816	12.323	4.990	6.217
HF/6-31G*	3.028	11.665	3.770	6.663
HF/6-31+G*	2.217	11.174	3.596	6.718
HF/6-31G**	2.569	9.332	5.343	6.096
HF/6-311++G**//6-31G**	1.987	8.729	5.226	5.808
MP2/6-31G*//HF/6-31G*	2.469	7.098	5.292	6.264

the solvent effect on the conformational equilibrium for the DCMU parent compound.

In the first part, the solvation process was considered using two different continuum models: the real cavity approach (IPCM) and the standard spherical cavity Onsager model (SCRF). The structural contribution to the solvation process was investigated through geometry optimizations in the presence of the reaction field (SCRF dipole model). In the SCRF approach only the dipole term was included in the electrostatic potential expansion and the IPCM calculations were carried out considering different isosurface levels. All the calculations were performed at the HF level using the 6-31G** optimized geometries and the dielectric constant of water ($\varepsilon = 78.54$).

The relative free energy and conformational distribution obtained in water solution for the DCMU

Table 4. Relative Gibbs free energy and conformational population at 298 K (in square brackets) for the distinct conformations of the DCMU molecule in water solution. The dipole moments (μ) obtained from the gas phase calculations are also reported

	ΔG (kcal/mol) [population]			
	A	B	C	D
HF/6-31G** (SCRF, dipole)[a,c]	−1.055 [86%]	0.000 [14%]	6.408 [0%]	6.364 [0%]
HF/6-31G** (SCRF, dipole)[b,c]	−1.048 [85%]	0.000 [15%]	6.483 [0%]	6.476 [0%]
HF/6-31G** (IPCM, 0.001)[d]	−6.292 [100%]	0.000 [0%]	0.266 [0%]	0.859 [0%]
HF/6-31G** (IPCM, 0.0005)[d]	−2.720 [99%]	0.000 [1%]	3.580 [0%]	3.492 [0%]
HF/6-31G** (IPCM, 0.0001)[d]	−1.810 [96%]	0.000 [4%]	5.114 [0%]	5.102 [0%]
HF/6-31G** (SM + SCRF, dipole)[e]	−1.432 [92%]	0.000 [8%]	3.278 [0%]	3.540 [0%]
HF/6-311++G**//6-31G* (SCRF, dipole)[a,c]	−1.106 [87%]	0.000 [13%]	6.105 [0%]	5.994 [0%]
HF/6-311++G**//6-31G** (IPCM, 0.001)[d]	−5.210 [100%]	0.000 [0%]	0.938 [0%]	0.973 [0%]
HF/6-311++G**//6-31G** (IPCM, 0.0005)[d]	−1.748 [95%]	0.000 [5%]	4.012 [0%]	3.894 [0%]
	μ (gas phase/Debye)			
	A	B	C	D
HF/6-31G**	7.578	5.895	2.612	2.727
HF/6-311++G**//6-31G**	7.553	5.907	2.734	2.773

[a] Values obtained using the gas phase optimized structures
[b] Values obtained using the aqueous optimized structures
[c] The cavity radii used were (in Å): 4.90 (A), 4.83 (B), 4.81 (C) and 4.61 (D)
[d] The values in parentheses specify the isosurface level (see [18])
[e] SM + SCRF stand for Super Molecule + SCRF continuum hybrid model. The cavity radii used for the DCMU…$(H_2O)_2$ complexes were (in Å): 5.26 ($A(H_2O)_2$), 5.15 ($B(H_2O)_2$), 5.25 ($C(H_2O)_2$) and 5.10 ($D(H_2O)_2$)

Table 5. Interconversion energy barriers (ΔE (TS_{ij})) obtained in water solution. The gas phase dipole moments are presented for the four transition state structures

	ΔE (TS_{ij}) (kcal/mol)			
	A → B	B → C	C → D	D → A
HF/6-31G** (SCRF, dipole)[a,b]	4.034	10.312	5.340	4.410
HF/6-31G** (IPCM, 0.001)[c]	2.266[d]	2.213[d]	2.119	7.173
HF/6-31G** (IPCM, 0.0005)[c]	2.157[d]	9.514[d]	1.895	7.405
HF/6-31G** (IPCM, 0.0001)[c]	4.265	10.363	3.440	5.836
HF/6-311++G**//6-31G** (SCRF, dipole)[a,b]	3.491	9.664	5.156	4.058
HF/6-311++G**//6-31G** (IPCM, 0.001)[c]	1.941[d]	6.871[d]	2.253	7.458
HF/6-311++G**//6-31G** (IPCM, 0.0005)[c]	1.601[d]	10.074[d]	2.349	6.627
	μ (gas phase/Debye)			
	TS_{AB}	TS_{BC}	TS_{CD}	TS_{DA}
HF/6-31G**	6.352	5.461	2.450	5.430
HF/6-311++G**//6-31G**	6.282	5.557	2.684	5.480

[a] Values obtained using the gas phase optimized structures
[b] The cavity radii used were (in Å): 4.94 (TS_{AB}), 5.18 (TS_{BC}), 4.63 (TS_{CD}) and 4.80 (TS_{DA})
[c] The values in parentheses specify the isosurface level (see [18])
[d] The transition state TS_{AB} has a lower energy value than conformer B

herbicide are presented in Table 4. In Table 5, the interconversion energy barriers calculated in the presence of the reaction field generated by the solvent are reported.

The values reported in Table 4 show that the *trans* conformation A corresponds to the lowest energy structure in aqueous medium. According to the SCRF continuum model, the relative concentration was found to be 86% (A) and 14% (B) (HF/6-31G**). The structural contribution to the solvation process was found not to be important to the conformational equilibrium (85% (A) and 15% (B)), the gas phase and water solution (SCRF) optimized structures being very similar. The improvement of the basis set does not significantly affect the relative energies obtained from the Onsager SCRF calculation, with the relative concentration of the A and B forms calculated to be 87% and 13% respectively.

The conformational distribution obtained from the IPCM calculation showed the *trans* form A in a relative concentration close to 100% in all methodologies em-

ployed. The decrease of the isodensity level slightly increases the population of the B form. The same effect is observed when the basis set is improved considering the same isodensity level; however the basis set effect is less pronounced. It can also be observed that the solvent effect obtained from the IPCM calculation is more significant than that predicted by the SCRF models. For the IPCM calculation with the isodensity level set to 0.001, the most nonpolar *cis* conformations were found to be less than 1 kcal/mol higher in energy than the *trans* polar form B. When the isodensity level is decreased from 0.001 to 0.0005 the relative energies change significantly. The calculated ΔG (A − B) values are −6.292 (0.001) and −2.720 kcal/mol (0.0005) at the HF/6-31G** level and −5.210 (0.001) and −1.748 kcal/mol (0.0005) using the HF/6-311 + + G**//6-31G** level of theory. As for the *trans* A form, the *cis* conformations C and D become less stable relative to B when the isodensity level is decreased. These results are explained better in Fig. 5, where the solvent effect on the relative free energy as a function of the dipole moment change is illustrated. The relative solvation free energy was calculated as $\Delta G^{solv} = \Delta G^{H_2O} - \Delta G^{gas}$, where the quantities ΔG^{H_2O} and ΔG^{gas} are the conformational free energy differences relative to form B presented in Tables 4 and 3 respectively. The relative dipole moment ($\Delta\mu$) was calculated using the gas phase values reported in Table 4 using conformer B as a reference. The negative values of ΔG^{solv} mean that the conformation considered is more stabilized relative to B in the presence of the solvent. In addition $\Delta G^{solv} > 0$ indicates a smaller stabilization relative to the form B. From a direct analysis of Fig. 5, it can be observed that the solvent effect on conformation A is more pronounced for the IPCM approach, ΔG^{solv} being equal to (in kcal/mol): −6.763 (IPCM, 0.001) and −1.526 (SCRF, dipole) for the HF/6–31G** calculations. At the HF/6-311 + + G**//6-31G** level the same trend is observed with ΔG^{solv} equal to −5.624 (IPCM, 0.001) and −1.520 kcal/mol (SCRF, dipole). Considering the positive value of $\Delta\mu$ (1.683 D and 1.646 D respectively for the HF/6-31G** and HF/6-311 + + G**//6-31G** levels), the stabilization solvent effect for conformer A follows the dipole moment variation in both continuum models, considering only the polarization solvent effect. The *cis* forms present negative values of $\Delta\mu$, −3.283 D and −3.168 D (HF/6-31G**) and −3.173 D and −3.134 D (HF/6-311 + + G**//6-31G**), respectively for C and D). Figure 5 shows a stabilization solvent effect from the IPCM (0.001) calculation, with ΔG^{solv} equal to −3.861 (C) and −3.338 kcal/mol (D) (HF/6-31G**) and −2.888 (C) and −2.840 kcal/mol (D) (HF/6-311 + + G**//6-31G**). Considering the values of $\Delta\mu$, the solvation energy does not follow the dipole moment change, as it is expected that a polar solute should be more stabilized in polar medium than nonpolar molecules. The solvent effect calculated from the SCRF approach is in agreement with this assumption: ΔG^{solv} (HF/6-31G**) = 2.281 (C) and 2.167 kcal/mol (D) and ΔG^{solv} (HF/6-311 + + G**//6-31G**) = 2.279 (C) and 2.181 kcal/mol (D).

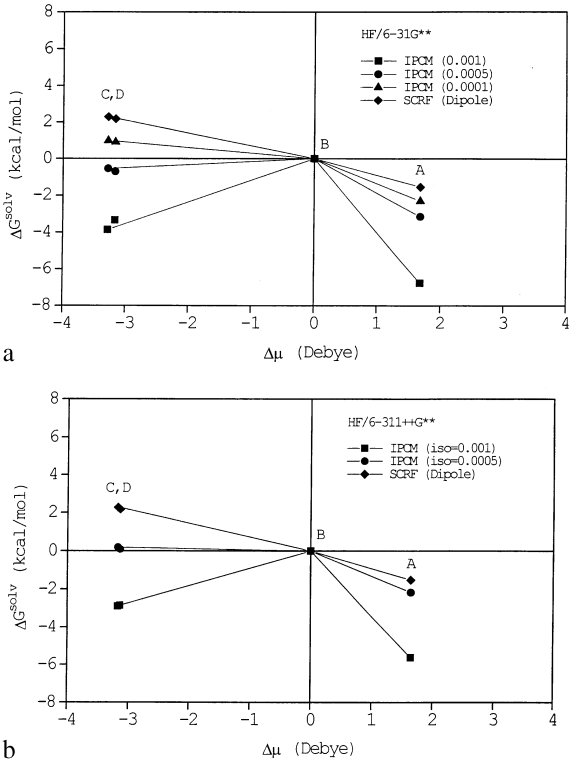

Fig. 5a,b. Solvent effect on the relative free energy. $\Delta\mu$ are calculated considering the *trans* conformation B as reference

The effect of decreasing the isodensity level in the IPCM model reported in Table 4 can be seen in Fig. 5. Analyzing the changes in the solvation free energies with the isodensity level, it can be observed that ΔG^{solv} seems to converge to a constant value for the same conformation and the upper limit should be close to the SCRF result. The choice of isodensity level in the IPCM model has been made arbitrarily and some authors have shown that a value of 0.0004 is a better choice [25–27]. In the present study, the isosurface level which defines the genuine solute cavity cannot be established directly from the analysis reported in Table 4 and Fig. 5, as the experimental solvent effect on the conformational equilibrium for the DCMU molecule has not been reported so far. However, according to studies reported for IPCM calculations [25–27], the results obtained from the IPCM (0.0005) should be considered as the most real continuum model for the molecules studied here.

In an attempt to obtain more realistic solvation energies, a hybrid discrete-continuum model was used. It was done considering the supermolecule obtained from process (1) and the free energy of solvation calculated according to Eq. (2) (see Sect. 2). The supermolecule geometries were fully optimized in the gas phase using the HF/6-31G** level of theory and the thermal correction to the free energy was calculated from the vibrational frequencies obtained at the same level of calculation.

The relative free energies are reported in Table 4, denoted as HF/6-31G** (SM + SCRF, dipole). The graph of ΔG^{solv} against $\Delta\mu$ is depicted in Fig. 6, where the results obtained from HF/6-31G** (IPCM, 0.0005) are included for comparison. Analyzing the values from Table 4, it can be seen that the relative free energies for

the forms C and D were found to be closer to the results obtained from the HF/6-31G** (IPCM, 0.0005). For the *trans* conformer A, the calculated relative free energy was −1.432 kcal/mol which is 1.3 kcal/mol higher than the value obtained from the HF/6–31G** (IPCM, 0.0005). The solvation energy for the form A calculated from the hybrid model was found to be −1.903 kcal/mol and that obtained from the HF/6-31G** calculations (IPCM, 0.0005) was equal to −3.137 kcal/mol (see Fig. 6). One possible reason to the small solvation energy in the supermolecule approach can be attributed to the polarization energy contribution evaluated from the SCRF continuum model [Eq. (2) in Sect. 2]. As mentioned before, the polarization effect of the solvent calculated from the IPCM model is more pronounced than that from the SCRF model. Considering conformation A, the calculated HF/6-31G** (IPCM, 0.0005) ΔG^{pol} was −11.375 kcal/mol and only −5.456 kcal/mol employing the supermolecule approach. However, it is important to make clear that the SM + SCRF hybrid model presented results which are closer to the IPCM model with the isosurface level 0.0005 being the best choice for the system and level of theory considered here. Another point, which should be raised here, is that, as obtained from the calculation in the gas phase, the results in water solution suggest that the *cis* conformers (C and D) should not be observed in the conformational mixture in a significant concentration.

The optimized geometries of the supermolecules ($DCMU_i \ldots (H_2O)_2$) are depicted in Fig. 7. The main

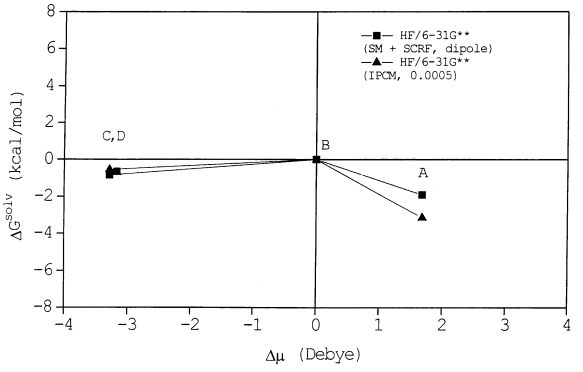

Fig. 6. Solvent effect on the relative free energy obtained from the hybrid discrete-continuum model. The values calculated using the HF/6-31G**(IPCM, 0.0005) are also presented for comparison. $\Delta\mu$ are calculated considering the *trans* conformation B as reference

Fig. 7a–d. HF/6-31G** optimized geometries for the $DCMU_i \ldots (H_2O)_2$ complexes. The hydrogen-bond length (in Å) and the dihedral angles between the phenyl ring and the dimethylurea moiety are reported: $A \ldots (H_2O)_2$; $w_\perp = -156.0°$, $w_{11} = -148.7°$(a), $B \ldots (H_2O)_2$; $w_\perp = -8.8°$, $w_{11} = -29.5°$(b), $C \ldots (H_2O)_2$; $w_\perp = 41.5°$, $w_{11} = 20.3°$(c), $D \ldots (H_2O)_2$; $w_\perp = 136.9°$, $w_{11} = 164.3°$

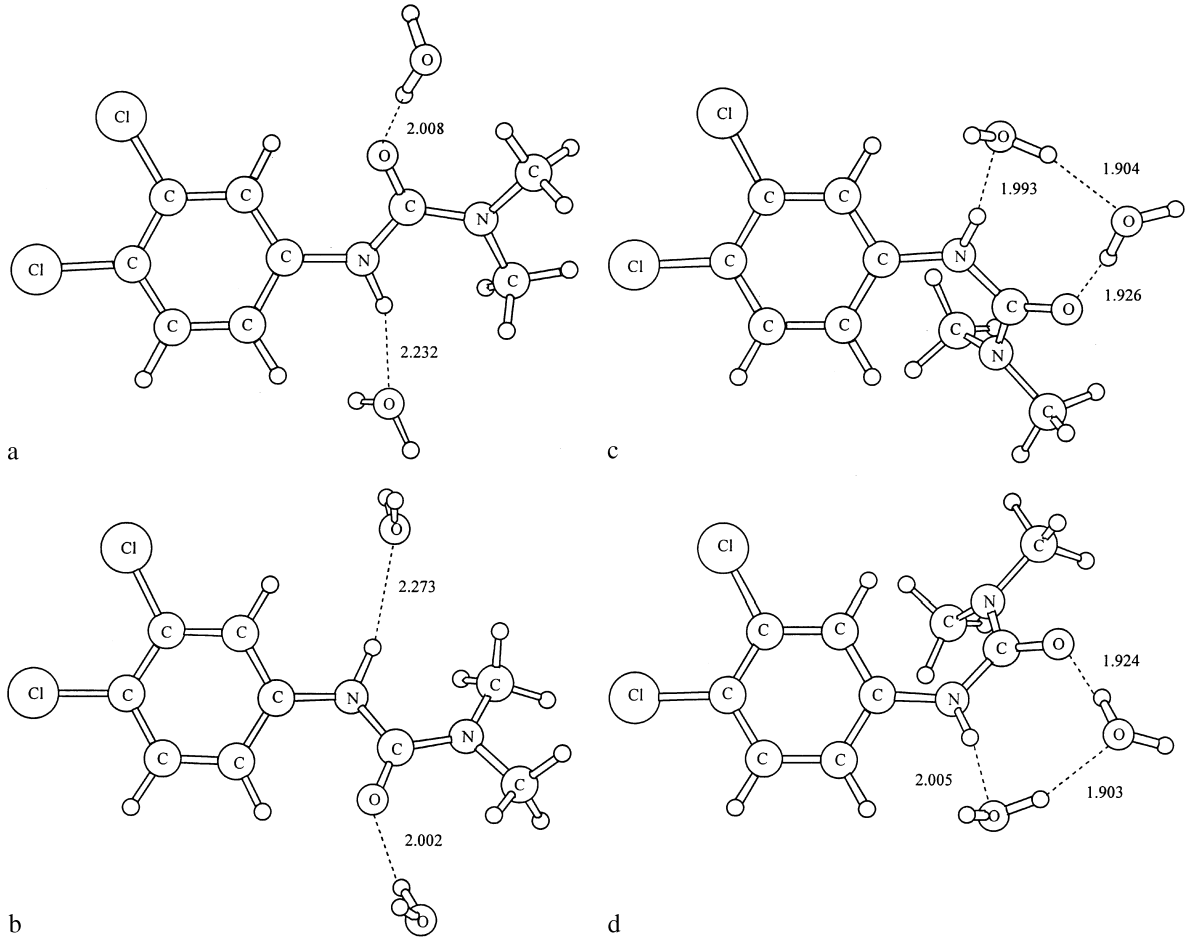

geometric parameters are also reported. It can be seen that the hydrogen bonds involving the A and B forms with the water molecules are energetically higher than those observed for the *cis* conformations. This could be one factor responsible for the stabilization solvent effects of the nonpolar *cis* conformations relative to the B form (see Figs. 5 and 6). In the C…$(H_2O)_2$ and D…$(H_2O)_2$ complexes, there is also a possibility of interaction between the two water molecules, which is favorable for the solvation process.

The hydrogen bond also affects the conformation. For the *trans* forms A and B a twisted structure was found in the supermolecule study. The phenyl ring and urea group were observed to be twisted by 31° (A) and 30° (B) (values of ω_{11}), showing that the nonplanar conformation obtained from the solid state is due to the presence of hydrogen bonds in the crystalline net, as discussed in the first part of this work.

Finally it is important to analyze the solvent effect on the rotational barriers. Table 5 reports the energy barriers for conformational interconversion processes 1–4 calculated using distinct continuum models. From the SCRF results it can be observed that processes A → B and B → C should be slower in the presence of the solvent at both levels of theory. The energy barrier for the interconversion C → D is slightly affected by the solvent. ΔE^{solv}, which is the difference between the energy barriers calculated in water solution (ΔE^{H_2O}, Table 5) and those obtained in the gas phase (ΔE^{gas}, Table 3), gave the values −0.003 (HF/6-31G**) and −0.070 kcal/mol (HF/6-311++G**//6-31G**), which are in agreement with a $\Delta\mu$ ($=\mu(TS_{ij}) - \mu_i$) value close to zero (see Tables 4, 5). Interconversion process D → A should occur faster in water solution than in the gas phase according to the SCRF calculations. $\Delta\mu$ were found to be 2.703 D and 2.707 D showing the dipole moment of TS_{DA} to be higher than form D, so the solvent effect should be greater for the transition state.

The IPCM calculations present some interesting results. In this approach, assuming the isodensity level is equal to 0.001, the transition state connecting the *trans* conformations (TS_{AB}) was found to be 4.18 (HF/6-31G**) and 3.42 kcal/mol (HF/6-311++G**//6-31G**) lower in energy than the *trans* form B. Considering the isosurface 0.0005, the same result was obtained with TS_{AB} being 0.66 (HF/6-31G**) and 0.30 kcal/mol (HF/6-31++G**/6-31G**) more stable than conformation B. Therefore, it can be said that conformer B, which is at the global minimum on the gas phase PES for the DCMU molecule, should not exist in aqueous media, when the solvent is included using the continuum IPCM model with the cavity set at 0.001 or 0.0005 isodensity. For the HF/6-31G** (IPCM, 0.0001), the result is reversed, conformer B being 2.30 kcal/mol more stable than the transition state TS_{AB}. Considering the results reported in the literature [25–27] and those presented in this work for the stable conformations A, B, C and D, it is expected that the values calculated from the IPCM model with the isodensity level equal to 0.0005 should be more reliable. Therefore, conformation B should promptly convert to the A form in water solution.

The energy barrier for the process C → D is 3.224 (HF/6-31G**, 0.001) 2.973 kcal/mol (HF/6-311++G**/6-31G**, 0.001) lower than that calculated in the gas phase, although $\Delta\mu \sim 0$. For the D → A interconversion process, the IPCM calculations showed a barrier of 7.173 and 7.458 kcal/mol at the HF/6-31G** and HF/6-311++G**//6-31G** level of theory (IPCM, 0.001) respectively, which are 1.077 and 1.650 kcal/mol higher than the value calculated in gas phase. This result does not follow the dipole moment change, as $\Delta\mu$ presented a positive value (2.703 D and 2.707 D).

From the results obtained in the gas phase and water solution, it can be concluded that the *trans* conformation A should be the most abundant form in polar media and the B conformer should be present in a nonpolar region of the organism. This is important because, as mentioned before, the partition coefficient is related to the herbicide activity, so the conformational interconversion process may play a role in the biological action. Additional studies have been developed with other phenyl-urea derivatives in order to access a quantitative relationship between structure and biological activity.

4 Conclusions

In the present study, we carried out an investigation of the conformational properties of the DCMU molecule, a photosystem II inhibitor, using high level ab initio methods in the gas phase and water solution. The solvent effect was included using the IPCM model and the standard Onsager SCRF continuum approach. The specific solute-solvent interactions were analyzed using hybrid discrete-continuum model.

The gas phase fully optimized geometries of the *trans* forms were found to be completely planar, which has been considered to be an important structural aspect for the herbicide binding. From the Gibbs population analysis, the *trans* conformations were predicted to be favorable in the ratio of 33% (A) and 67% (B) (HF/6-311++G**//6-31G**) and 38% (A) and 50% (B) (MP2/6-31G*//HF/6-31G*). At the MP2/6-31G*//HF/6-31G* level, the *cis* forms are present in the equilibrium mixture in a relative concentration of 6% (C) and 6% (D). The solid state structure exhibited a twisted geometry similar to the *trans* conformer B. The twisting was explained based on the weak intermolecular hydrogen bonds between the NH and C=O groups present in the crystalline net (O…N = 2.936 Å). The small energy difference between the twisted and the planar (B) forms (0.327 kcal/mol, HF/6-31G**) can be used to explain the twisting observed in the solid state.

The *trans* → *trans* interconversion process showed an energy barrier of only 2.5 kcal/mol at the MP2/6-31G*//6-31G* level of theory, this value being higher in the lowest level of calculation (HF/3-21G*, 5.8 kcal/mol). This result suggests that a flip-flop can be established between the *trans* conformations (A and B). However, for the *trans* → *cis* process B → C), the lowest value calculated for the energy barrier was found to be 7.098 kcal/mol (MP2/6-31G*//HF/6-31G*), which is high enough to avoid the interconversion process. A

corresponding process has been used to explain the reduction in the herbicide activity of the Swep derivative. For this compound, the energy barrier *cis* → *trans* was reported to be only 2.5 kcal/mol)

In water solution, the *trans* conformation A was found to be the most abundant form, with the relative concentration calculated to be close to 100% (IPCM) and 88% (SCRF). For the IPCM calculations, the decrease in the isodensity level from 0.001 to 0.0005 slightly increases the population of form B from 0% to 1% at the HF/6-31G** level and from 0% to 5% at the HF/6-311 + + G**//6-31G** level of theory. The hybrid model showed a conformational distribution of 92% (A) and 8% (B) which is in best agreement with the IPCM model with the solute cavity set to an isodensity level equal to 0.0005.

Considering the biological action of the urea-type herbicides, the results presented are important because, as has been mentioned, the partition coefficient is related to the herbicide activity, so the conformational equilibrium (A → B) may play a role in the biological action. Another interesting result is that form B does not exist in water solution according to the IPCM (0.0005) calculations, so conformation B should be present in a non-polar region of the organism and it promptly converts to the A form in aqueous media.

Acknowledgements. H.F. Dos Santos thanks the CNPq (Conselho Necional de Desenvolvimento Científico e Tecnológico) for a research grant. W.B. De Almeida would like to thank the Fundação de Amparo a Pesquisa do Estado de Minas Gerais (FAPEMIG) and the Programa de Apoio ao Desenvolvimento Científico e Tecnológico (PADCT-Proc. No 62.0241/95.0) for supporting this project. The authors also thank the CENAPAD-MG/CO (Centro Nacional de Processamento de Alto Desempenho do Estado de Minas Gerais e Região Centro Oeste) for providing computer facilities. Finally, we would like to thank the referee for carefully reading the manuscript.

References

1. Voet D, Voet JG (1995) Biochemistry, 2nd edn. Wiley, New York
2. Michel H, Deisenhofer J (1988) Biochemistry 27:1
3. Trebst A, Hilp U, Draber W (1993) Phytochemistry 33:969
4. Deisenhofer J, Epp O, Miki K, Huber R, Michel H (1985) Nature 318:618
5. Bowyer J, Hilton M, Whitelegge J, Jewess P, Camilleri P, Crofts A, Robinson H (1990) Z Naturforsch 45c:379
6. Draber W, Tietjen K, Kluth JF, Trebst A (1991) Angew Chem Int Ed Engl 30:1621
7. Sinning I (1992) Trends Biochem Sci 17:150
8. Hansch C, Leo A (1995) Exploring QSAR, fundamentals and applications. In: Chemistry and biology. ACS professional reference book. American Chemical Society, Washington, DC, pp. 459
9. Kubinyi H (1993) QSAR: Hansch analysis and related approaches. VCH, New York
10. Karelson MM, Labanov VS, Katritzky AR (1996) Chem Rev 96:1027
11. De Almeida WB, O'Malley PJ (1992) Theochem 253:349
12. De Almeida WB, Dos Santos HF, O' Malley PJ (1995) Struct Chem 6:383
13. Silva THA, Oliveira AB, De Almeida WB (1997) Struct Chem 8:95
14. Silva THA, Oliveira AB, De Almeida WB (1997) Bioorg Med Chem 5:353
15. Dos Santos HF, De Almeida WB, Zerner MC (1998) J Pharm Sci 87:190
16. Trebst A, Donner W, Draber W (1984) Z Naturforsch 39c:405
17. Creuzet S, Gilquin B, Ducruet JM (1989) Z Naturforsch 44c:435
18. Foresman JB, Keith TA, Wiberg KB, Snoonian J, Frish MJ (1996) J Phys chem 100:16098
19. Onsager L (1936) J Am Chem Soc 58:1486
20. Szafran M, Karelson MM Kartrizky AR, Koput J, Zerner MC (1993) J Comp Chem 14:371
21 Li G-S, Ruiz-López MF, Maigret B (1997) J Phys Chem 101:7885
22. Cramer CJ, Truhlar DG (1992) J Comput Aided Mol Des 6:629
23. Frisch MJ, Trucks GW, Schlegel HB, Gill PMW, Johnson BG, Robb MA, Cheeseman JR, Keith T, Petersson GA, Montgomery JA, Raghavachari K, Al-Laham MA, Zakrzewski VG, Ortiz JV, Foresman JB, Cioslowski J, Stefanov BB, Nanayakkara A, Challacombe M, Peng CY, Ayala PY, Chen W, Wong MW, Andres JL, Replogle ES, Gomperts R, Martin RL, Fox DJ, Binkley JS, Defrees DJ, Baker J, Stewart JJP, Head-Gordon M, Gonzalez C, Pople JA (1995) Gaussian 94, revision D.2. Gaussian, Pittsburgh, PA
24. Pfefer G, Boistelle R (1996) Acta Crystallogr B52:662
25. Wiberg KB, Keith TA, Frisch MJ, Murcko M (1995) J Phys Chem 99:9072
26. Wiberg KB, Rablen PR, Rush DJ, Keith TA (1995) J Am Chem Soc 117:4261
27. Wiberg KB, Castejon H (1996) J Comput Chem 17:185
28. Pople JA, Scott AP, Wong MW, Radom L (1993) Isr J Chem 33:345